



The trapping of surface waves by multiple submerged horizontal cylinders

R. PORTER and D. V. EVANS

School of Mathematics, University of Bristol, Bristol BS8 1TW, UK; e-mail: richard.porter@bristol.ac.uk

Received 2 October 1997; accepted in revised form 31 July 1998

Abstract. The existence of edge waves, or trapped modes, travelling above a single long horizontal submerged cylinder is well established in the linearised theory of water waves. In the present paper, the possibility of wave-trapping by multiple submerged horizontal circular cylinders is considered. The trapped mode solutions are constructed by means of a multipole approach combined with an addition formula for Bessel functions and requires finding the non-trivial solutions of a real infinite system of algebraic equations. The case of a single submerged cylinder is returned to briefly, where results for symmetric trapped modes are reproduced and new numerical results for antisymmetric modes are presented. A large range of results are also presented for multiple cylinders.

Key words: trapping, waves, cylinders, submerged, multiple.

1. Introduction

In 1846 Stokes produced a simple solution to the linearized water wave equations which represented a wave travelling in the long-shore direction over a uniformly sloping beach. This solution, now called an edge wave, decays in the direction of increasing depth and exists for all beach angles β provided that the long-shore wavenumber k is related to the wave frequency $\omega/2\pi$, through the relation $\omega^2 = gk \sin \beta$. It was not until over a century later that a further localized solution was discovered by Ursell [1]. He proved, using multipole expansions and infinite determinants, that there existed a wave travelling along the top of a totally submerged horizontal cylinder of infinite extent, in infinitely-deep water. The solution decays with horizontal distance away from the cylinder axis and exists for a particular relation between its wavelength and frequency depending on its radius and depth of submergence. Ursell's proof required the radius of the cylinder to be sufficiently small. This restriction was removed by Jones [2] who proved, using deep results from the theory of unbounded operators, that such trapped modes existed for a wide class of submerged infinitely-long horizontal cylinders which are symmetric about the vertical axis. A simpler proof based on potential theory and comparison theorems was later provided by Ursell [3]. For a description of recent work on trapped modes above submerged bodies in more general situations, see Evans and Kuznetsov [4].

The method used by Ursell for the submerged horizontal circular cylinder was to construct a solution in terms of an infinite series of multipoles each of which satisfied all the conditions of the problem except for the Neumann condition on the surface of the cylinder. Application of this condition resulted in a homogeneous real infinite system of equations for the Fourier coefficients in the multipole expansion. By an ingenious double-limit procedure, he was able

to show that the infinite determinant of this system vanished for a particular relation between frequency and wavelength along the top of the cylinder provided the cylinder was sufficiently small. In 1985 McIver and Evans [5] revisited the problem and sought solutions by computing the real zeros of the infinite determinant for all parameter values. They found that for a cylinder of arbitrary size, there was always at least one trapped mode as is guaranteed by the existence proofs of [2] and [3]. However, they also found that as the highest point of the cylinder approached the free surface, further trapped modes occurred, each mode having a distinct relationship between frequency and wavelength along the cylinder. The modes were all, by construction, symmetric about a vertical plane through the axis of the cylinder.

In the present paper, we generalize the problem by considering possible trapped modes in the presence of any number of distinct, non-overlapping totally submerged infinitely-long circular cylinder of any size and placed in any position. The authors are not aware of any previous results for trapped modes over multiple submerged bodies. However, the method, which involves the use of Graf's addition formulae for Bessel functions to shift co-ordinates between cylinders, has been used by recently by Linton and McIver [8] to consider the scattering of waves by any number of bottom-mounted *vertical* cylinders in a channel. More pertinently, the present authors have used the technique to consider the possible trapped modes in the vicinity of any number of bottom-mounted vertical cylinders positioned on the centre-plane of a channel. Thus it was found (Evans and Porter [7]) that in general the number of trapped modes for a given geometry was the same as the number of cylinders present and each mode approaches a unique mode for a single cylinder as the spacing between the cylinders increased. We expect to find a similar behaviour in the present case of any number of submerged horizontal cylinders but the situation is more complicated by the fact that even for a single horizontal cylinder, the number of trapped modes depends critically upon its depth of submergence. Again it will be possible to explore the effect on the trapped modes of varying both size and position of the cylinders. This was not possible in the case of the vertical cylinders in the channel since in order to guarantee the occurrence of trapped modes the cylinders had to remain on the centre-plane of the channel.

The plan of the paper is as follows. The problem is formulated in Section 2 where the infinite system of equations is derived for the general case using results developed in the Appendices. Some special cases are considered which reduce the complexity of the system through symmetry. These include all cylinders lying in the same vertical plane when the system decouples into a symmetric and an antisymmetric system and two identical equally-submerged cylinders, where the system reduce to two systems describing either even or odd solutions about the vertical plane mid-way between the cylinders. The case of a single cylinder is readily deduced from the general formulation and takes the form of two decoupled systems for symmetric and antisymmetric solutions. The former was the system computed by McIver and Evans [5] but the latter system is new and computations in Section 3 confirm the existence of antisymmetric solutions for a single cylinder sufficiently close to the free surface. Such antisymmetric solutions were earlier reported by Martin [6] using a boundary integral equation based on Green's theorem. He obtained antisymmetric solutions above both circular and elliptic cylinders. A variety of results are presented in Section 3. For the case of two identical cylinders of radius a , these include curves showing the variation of K/k with ka for trapped modes for the given geometry. Here $K = \omega^2/g$, and k is the wavenumber in the direction of the axis of the cylinders. Also investigated is the variation of K/k as cylinders are moved apart from one another where we expect the results to converge to those for single cylinders in isolation.

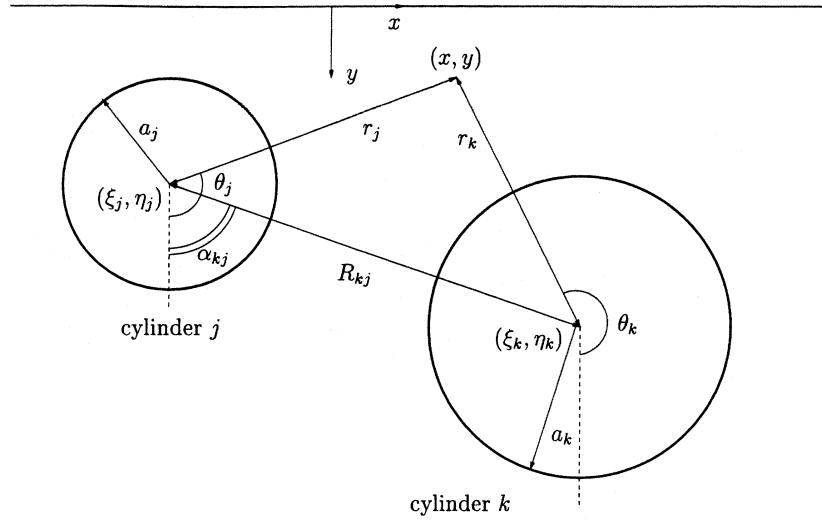


Figure 1. General configuration of submerged cylinders.

2. Formulation and solution

The solution to the classical linearized water wave equations may be expressed in terms of a three-dimensional time-dependent velocity potential, $\Phi(x, y, z, t)$ which we may write in the form

$$\Phi(x, y, z, t) = \text{Re}\{\phi(x, y) e^{i(kz - \omega t)}\}, \quad (2.1)$$

where we assume time-harmonic motion of angular frequency ω and a periodicity in the z -direction having an associated wavenumber k . We choose Cartesian co-ordinates with x, z lying in the undisturbed free surface and y vertically downwards. The two-dimensional function $\phi(x, y)$ now satisfies the following boundary-value problem

$$(\nabla^2 - k^2)\phi = 0, \quad \text{in the fluid, outside the cylinder,} \quad (2.2)$$

$$K\phi + \phi_y = 0, \quad \text{on } y = 0, \quad (2.3)$$

where $K = \omega^2/g$ and g is the acceleration due to gravity. Physically, the decomposition in (2.1) describes a wave travelling parallel to the cylinders with a wavenumber k parallel to the z -coordinate. In the corresponding scattering problem, an incident wave of wavenumber K making an angle θ to the cylinders gives $k = K \sin \theta$ and clearly $K > k$. This provides a cut-off wavenumber $K = k$, and choosing $K < k$ in the absence of an incident wave field implies that waves cannot radiate to $x = \pm\infty$. Thus, for $K < k$,

$$\phi \rightarrow 0, \quad \text{as } |x| \rightarrow \infty, \quad (2.4)$$

whilst

$$\nabla\phi \rightarrow 0, \quad \text{as } y \rightarrow \infty, \quad (2.5)$$

$$\phi_n = 0, \quad \text{on the surface of each cylinder,} \quad (2.6)$$

where n denotes the normal derivative, completes the boundary-value problem.

The configuration consists of N cylinders, the centre of cylinder j placed at (ξ_j, η_j) and with radius a_j ($j = 1, \dots, N$) such that all cylinders are submerged and no two cylinders intersect. We define local polar coordinates, (r_j, θ_j) about the centre of each cylinder by

$$\begin{aligned} x &= \xi_j + r_j \sin \theta_j, \\ y &= \eta_j + r_j \cos \theta_j, \end{aligned} \quad (2.7)$$

so that angles are measured anti-clockwise and with respect to the downward vertical. Also worth defining at this stage is

$$R_{kj} = \{(\xi_k - \xi_j)^2 + (\eta_k - \eta_j)^2\}^{1/2}, \quad R_{jk} = R_{kj}, \quad (2.8)$$

$$\alpha_{kj} = \tan^{-1} \left(\frac{\xi_k - \xi_j}{\eta_k - \eta_j} \right), \quad \alpha_{jk} = \pi + \alpha_{kj} \quad (2.9)$$

being the relative distance and orientation between cylinders j and k as shown in Figure 1.

The fundamental solution to (2.2) having a singularity at the centre of cylinder j is $K_n(kr_j) e^{in\theta_j}$. The modification to these singular solutions satisfying (2.3) are the so-called multipoles derived in Appendix A. Thus from (A.8) we define $\phi_n^j(r_j, \theta_j) = \varepsilon_n \operatorname{Re}\{w_n(r_j, \theta_j)\}$ and $\psi_n^j(r_j, \theta_j) = \varepsilon_n \operatorname{Im}\{w_n(r_j, \theta_j)\}$ and so

$$\begin{aligned} \phi_n^j(r_j, \theta_j) &= \varepsilon_n K_n(kr_j) \cos n\theta_j + \varepsilon_n (-1)^n \\ &\quad \times \int_0^\infty \frac{k \cosh t + K}{k \cosh t - K} e^{-k(y+\eta_j) \cosh t} \cosh nt \cos\{k(x - \xi_j) \sinh t\} dt \end{aligned} \quad (2.10)$$

and

$$\begin{aligned} \psi_n^j(r_j, \theta_j) &= \varepsilon_n K_n(kr_j) \sin n\theta_j - \varepsilon_n (-1)^n \\ &\quad \times \int_0^\infty \frac{k \cosh t + K}{k \cosh t - K} e^{-k(y+\eta_j) \cosh t} \sinh nt \sin\{k(x - \xi_j) \sinh t\} dt \end{aligned} \quad (2.11)$$

satisfying (2.2)–(2.5). It is convenient to introduce the factor ε_n defined by $\varepsilon_0 = 1$, $\varepsilon_n = 2$, for $n \geq 1$, though redundant in (2.11) since $\psi_0^j \equiv 0$; its purpose becomes clear later in the paper. The real symmetric and antisymmetric multipoles in (2.10) and (2.11) above (respectively) are the building blocks of the solution since we now write the full potential as

$$\phi(x, y) = \sum_{j=1}^N \sum_{n=0}^{\infty} \{A_n^j \phi_n^j(r_j, \theta_j) + B_n^j \psi_n^j(r_j, \theta_j)\} \quad (2.12)$$

being the sum over all cylinders and all multipoles, with A_n^j , B_n^j coefficients to be determined ($B_0^j = 0$ is assumed). This is achieved by imposing the remaining condition (2.6) of no-flow on the cylinder bodies, written more precisely as

$$\left. \frac{\partial \phi}{\partial r_k} \right|_{r_k=a_k} = 0, \quad k = 1, \dots, N. \quad (2.13)$$

In order to impose this condition, it is necessary to express the potential in terms of local polar coordinates (r_k, θ_k) only. This requires shifting the coordinates from cylinder j to cylinder k in (2.10) and (2.11) above. Thus, using (B.2), (B.3), (B.12) and (B.13) from Appendix B, we obtain

$$\phi_n^k(r_k, \theta_k) = \varepsilon_n K_n(kr_k) \cos n\theta_k + \sum_{m=0}^{\infty} I_m(kr_k) c_{mn}^{kk} \cos m\theta_k \quad (2.14)$$

$$\begin{aligned} &= \sum_{m=0}^{\infty} I_m(kr_k) \{ (C_{mn}^{kj} + c_{mn}^{kj}) \cos m\theta_k \\ &\quad + (D_{mn}^{kj} + d_{mn}^{kj}) \sin m\theta_k \}, \quad j \neq k, \end{aligned} \quad (2.15)$$

$$\psi_n^k(r_k, \theta_k) = \varepsilon_n K_n(kr_k) \sin n\theta_k + \sum_{m=0}^{\infty} I_m(kr_k) f_{mn}^{kk} \sin m\theta_k \quad (2.16)$$

$$\begin{aligned} &= \sum_{m=0}^{\infty} I_m(kr_k) \{ (E_{mn}^{kj} + e_{mn}^{kj}) \cos m\theta_k \\ &\quad + (F_{mn}^{kj} + f_{mn}^{kj}) \sin m\theta_k \}, \quad j \neq k, \end{aligned} \quad (2.17)$$

where C_{mn}^{kj} , D_{mn}^{kj} , E_{mn}^{kj} and F_{mn}^{kj} are defined in (B.4)–(B.7) and where

$$\begin{aligned} c_{mn}^{kj} &= \varepsilon_n \varepsilon_m (-1)^{m+n} \int_0^{\infty} \frac{k \cosh t + K}{k \cosh t - K} e^{-k(\eta_k + \eta_j) \cosh t} \\ &\quad \times \cosh nt \cosh mt \cos\{k(\xi_k - \xi_j) \sinh t\} dt, \end{aligned} \quad (2.18)$$

$$\begin{aligned} d_{mn}^{kj} &= \varepsilon_n \varepsilon_m (-1)^{m+n} \int_0^{\infty} \frac{k \cosh t + K}{k \cosh t - K} e^{-k(\eta_k + \eta_j) \cosh t} \\ &\quad \times \cosh nt \sinh mt \sin\{k(\xi_k - \xi_j) \sinh t\} dt, \end{aligned} \quad (2.19)$$

$$\begin{aligned} e_{mn}^{kj} &= -\varepsilon_n \varepsilon_m (-1)^{m+n} \int_0^{\infty} \frac{k \cosh t + K}{k \cosh t - K} e^{-k(\eta_k + \eta_j) \cosh t} \\ &\quad \times \sinh nt \cosh mt \sin\{k(\xi_k - \xi_j) \sinh t\} dt, \end{aligned} \quad (2.20)$$

$$\begin{aligned} f_{mn}^{kj} &= \varepsilon_n \varepsilon_m (-1)^{m+n} \int_0^{\infty} \frac{k \cosh t + K}{k \cosh t - K} e^{-k(\eta_k + \eta_j) \cosh t} \\ &\quad \times \sinh nt \sinh mt \cos\{k(\xi_k - \xi_j) \sinh t\} dt. \end{aligned} \quad (2.21)$$

We may now expand the total potential about the k th cylinder, thus

$$\begin{aligned} \phi(r_k, \theta_k) &= \sum_{n=0}^{\infty} \left\{ \varepsilon_n K_n(kr_k) \{ A_n^k \cos n\theta_k + B_n^k \sin n\theta_k \} \right. \\ &\quad \left. + \sum_{m=0}^{\infty} I_m(kr_k) \{ A_n^k c_{mn}^{kk} \cos m\theta_k + B_n^k f_{mn}^{kk} \sin m\theta_k \} \right\} \end{aligned}$$

$$\begin{aligned}
& + \sum_{j=1}^N \sum_{n=0}^{\infty} \sum_{\substack{m=0 \\ \neq k}}^{\infty} I_m(kr_k) \{ A_n^k ((C_{mn}^{kj} + c_{mn}^{kj}) \cos m\theta_k + (D_{mn}^{kj} + d_{mn}^{kj}) \sin m\theta_k) \\
& + B_n^k ((E_{mn}^{kj} + e_{mn}^{kj}) \cos m\theta_k + (F_{mn}^{kj} + f_{mn}^{kj}) \sin m\theta_k) \}. \tag{2.22}
\end{aligned}$$

Application of the body-boundary condition, (2.13), and use of the orthogonality of $\{\cos m\theta_k, \sin m\theta_k\}$, $m = 0, 1, \dots$, results in the following coupled systems of linear equations

$$\begin{aligned}
& \varepsilon_m K'_m(ka_k) A_m^k + I'_m(ka_k) \sum_{n=0}^{\infty} A_n^k c_{mn}^{kk} \\
& + I'_m(ka_k) \sum_{\substack{j=1 \\ \neq k}}^N \sum_{n=0}^{\infty} \{ A_n^j (C_{mn}^{kj} + c_{mn}^{kj}) + B_n^j (E_{mn}^{kj} + e_{mn}^{kj}) \} = 0, \tag{2.23}
\end{aligned}$$

$$\begin{aligned}
& \varepsilon_m K'_m(ka_k) B_m^k + I'_m(ka_k) \sum_{n=0}^{\infty} B_n^k f_{mn}^{kk} \\
& + I'_m(ka_k) \sum_{\substack{j=1 \\ \neq k}}^N \sum_{n=0}^{\infty} \{ A_n^j (D_{mn}^{kj} + d_{mn}^{kj}) + B_n^j (F_{mn}^{kj} + f_{mn}^{kj}) \} = 0, \tag{2.24}
\end{aligned}$$

where in both cases $k = 1, \dots, N$ and $m = 0, 1, \dots$. In practice, we truncate the infinite system at $n = M$, using the fact that $B_0^j = 0$, to leave a $N(2M + 1) \times N(2M + 1)$ linear system of algebraic equations.

2.1. A NOTE ON EFFICIENT NUMERICAL COMPUTATIONS

In order to compute (2.23), (2.24), we can take advantage of various symmetries involving the coefficients. This was made possible by introducing the factor ε_n in the definition of the multipoles in (2.10), (2.11). Thus, it is noted that

$$\begin{aligned}
C_{mn}^{kj} &= C_{nm}^{kj} = (-1)^{m+n} C_{mn}^{jk}, & c_{mn}^{kj} &= c_{nm}^{kj} = c_{mn}^{jk}, \\
D_{mn}^{kj} &= E_{nm}^{kj} = (-1)^{m+n} D_{mn}^{jk}, & d_{mn}^{kj} &= -e_{nm}^{kj} = -d_{mn}^{jk}, \\
E_{mn}^{kj} &= D_{nm}^{kj} = (-1)^{m+n} E_{mn}^{jk}, & e_{mn}^{kj} &= -d_{nm}^{kj} = -e_{mn}^{jk}, \\
F_{mn}^{kj} &= F_{nm}^{kj} = (-1)^{m+n} F_{mn}^{jk}, & f_{mn}^{kj} &= f_{nm}^{kj} = f_{mn}^{jk}.
\end{aligned}$$

2.2. CYLINDERS WITH CENTRES ALL LYING IN THE SAME VERTICAL PLANE

If the centres of all N cylinders lie in a vertical plane then a further simplification to the system (2.23), (2.24) can be made. In this case, $\xi_k = \xi_j$ and $\alpha_{kj} = 0$ or π for all j, k . This implies

$D_{mn}^{kj} = E_{mn}^{kj} = d_{mn}^{kj} = e_{mn}^{kj} = 0$ for all m, n, k, j . As a result, the two systems (2.23), (2.24) decouple into systems for A_n^j and B_n^j .

$$\varepsilon_m K'_m(ka_k) A_m^k + I'_m(ka_k) \sum_{n=0}^{\infty} A_n^k c_{mn}^{kk} + I'_m(ka_k) \sum_{\substack{j=1 \\ \neq k}}^N \sum_{n=0}^{\infty} A_n^j (C_{mn}^{kj} + c_{mn}^{kj}) = 0, \quad (2.25)$$

$$\varepsilon_m K'_m(ka_k) B_m^k + I'_m(ka_k) \sum_{n=0}^{\infty} B_n^k f_{mn}^{kk} + I'_m(ka_k) \sum_{\substack{j=1 \\ \neq k}}^N \sum_{n=0}^{\infty} B_n^j (F_{mn}^{kj} + f_{mn}^{kj}) = 0. \quad (2.26)$$

This is to be expected, since the geometric symmetry induced by placing all cylinders on the same vertical plane necessarily gives rise to a solution consisting of a linear combination of uncoupled pure symmetric and antisymmetric modes which are described by the coefficients A_n^j and B_n^j , respectively.

2.3. THE SINGLE CYLINDER SOLUTION

For purposes of comparison with multiple cylinders we will be concerned also with the trapped mode solution in the case of a single isolated cylinder of radius $a = a_1$ submerged to $\eta = \eta_1$. This is readily available from the general N -cylinder formulation by taking, unsurprisingly, $N = 1$. Then the systems (2.23), (2.24) decouple into the symmetric and antisymmetric trapped mode solutions

$$\varepsilon_m K'_m(ka) A_m^1 + I'_m(ka) \sum_{n=0}^{\infty} A_n^1 c_{mn}^{11} = 0, \quad m = 0, 1, 2, \dots \quad (2.27)$$

and

$$\varepsilon_m K'_m(ka) B_m^1 + I'_m(ka) \sum_{n=1}^{\infty} B_n^1 f_{mn}^{11} = 0, \quad m = 1, 2, \dots, \quad (2.28)$$

which can again be solved numerically by truncation to a size M .

2.4. TWO IDENTICAL EQUALLY SUBMERGED CYLINDERS

Take two identical cylinders submerged to the same depth such that $a = a_1 = a_2$, $\eta = \eta_1 = \eta_2$ and $\xi_1 = -\xi_2$. Then $x = 0$ is a line of geometric symmetry between the two cylinders about which the potential is either a symmetric (even) or an antisymmetric (odd) function. In this case the system (2.23), (2.24) simplifies in the following way.

An even/odd solution implies $\phi(x, y) = \pm\phi(-x, y)$ respectively. From (2.12) this requires

$$0 = \sum_{n=0}^{\infty} \{A_n^1 \phi_n^1(r_1, \theta_1) + B_n^1 \psi_n^1(r_1, \theta_1)\} \pm \{A_n^2 \phi_n^2(r_1, 2\pi - \theta_1) + B_n^2 \psi_n^2(r_1, 2\pi - \theta_1)\}, \quad (2.29)$$

whilst from (2.14), (2.16) it is easily verified that $\phi_n^2(r_1, 2\pi - \theta_1) = \phi_n^1(r_1, \theta_1)$ and $\psi_n^2(r_1, 2\pi - \theta_1) = -\psi_n^1(r_1, \theta_1)$. Thus, (2.29) reduces to

$$\left. \begin{aligned} A_n^1 &= \mp A_n^2 \\ B_n^1 &= \pm B_n^2 \end{aligned} \right\} \quad \forall n, \quad \text{for even/odd solutions}$$

and this simplifies (2.23), (2.24) to

$$\varepsilon_m K'_m(ka) A_m^1 + I'_m(ka) \sum_{n=0}^{\infty} \{A_n^1 (c_{mn}^{11} \mp (C_{mn}^{12} + c_{mn}^{12})) \pm B_n^1 (E_{mn}^{12} + e_{mn}^{12})\} = 0, \quad (2.30)$$

with

$$\varepsilon_m K'_m(ka) B_m^1 + I'_m(ka) \sum_{n=0}^{\infty} \{B_n^1 (f_{mn}^{11} \pm (F_{mn}^{12} + f_{mn}^{12})) \mp A_n^1 (D_{mn}^{12} + d_{mn}^{12})\} = 0, \quad (2.31)$$

where the upper (lower) sign refers to an even (odd) potential.

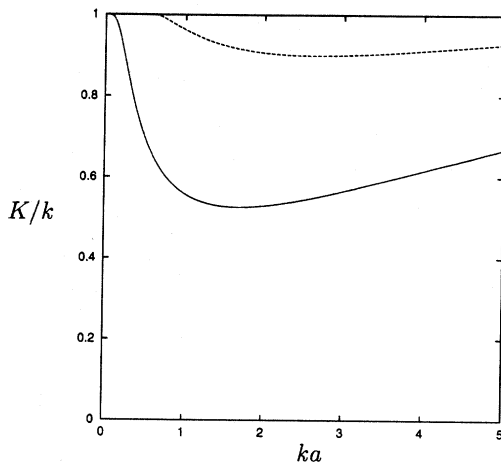


Figure 2. Curves showing the dispersion relation for the symmetric (—) and antisymmetric (---) modes when $\eta/a = 1.10$.

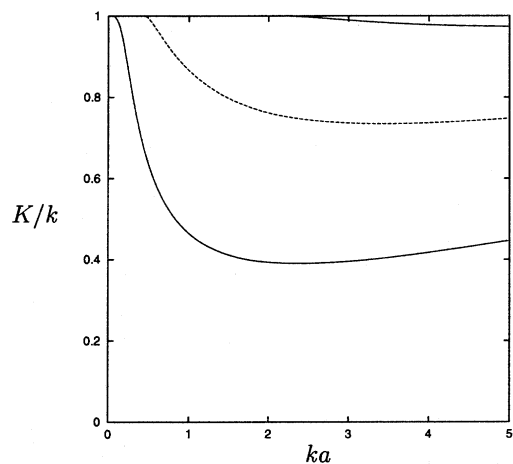


Figure 3. Curves showing the dispersion relation for the symmetric (—) and antisymmetric (---) modes when $\eta/a = 1.05$.

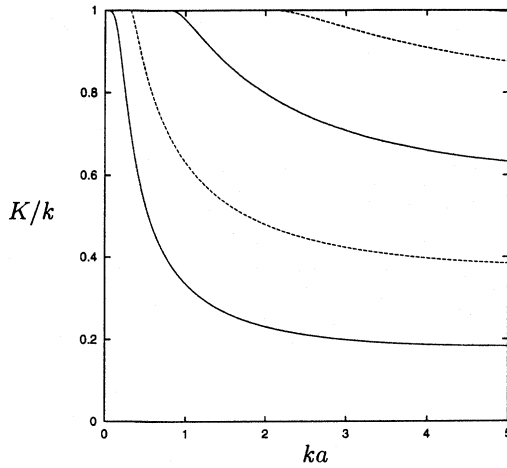


Figure 4. Curves showing the dispersion relation for the symmetric (—) and antisymmetric (- - -) modes when $\eta/a = 1.01$.

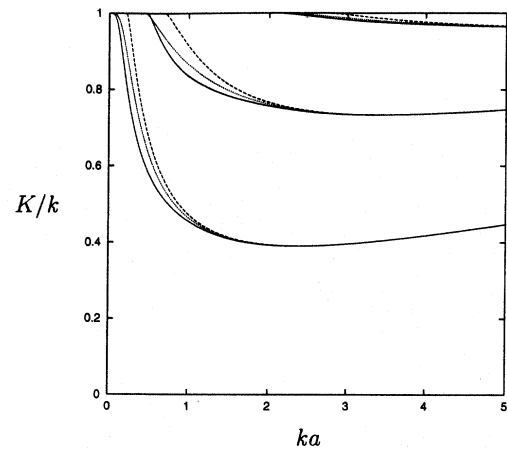


Figure 6. Curves showing the dispersion relation for the symmetric (—) and antisymmetric (- - -) modes for two equal cylinders with $\eta/a = 1.05$ and $\lambda = 2$. Dotted lines represent single cylinder results.

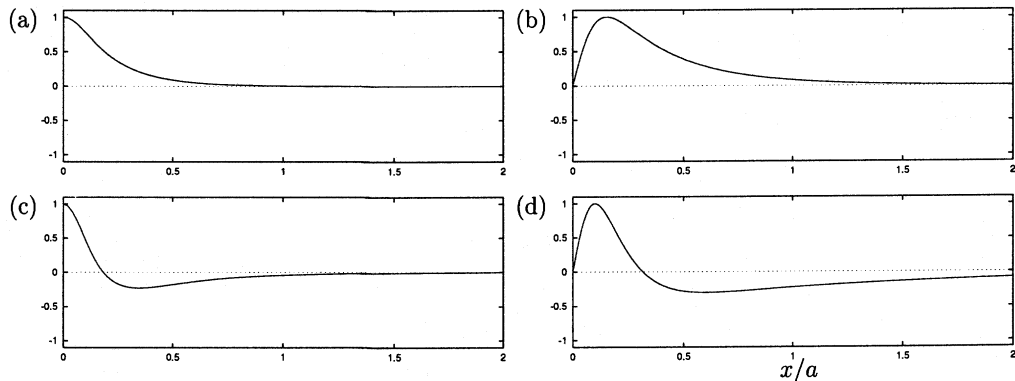


Figure 5. The free surface elevation corresponding to the four trapped modes present at $ka = 3$ and for $\eta/a = 1.01$. (a) first symmetric, (b) first antisymmetric, (c) second symmetric (d) second antisymmetric.

3. Results and discussion

3.1. THE SINGLE CYLINDER

The computation of the trapped modes requires that the infinite system (2.23) (or (2.24) in the case of antisymmetric modes) be truncated to a size, M , say. This must be chosen carefully to ensure adequate convergence, and it was found (as in [5]) that a larger truncation size was needed as the cylinder moved closer to the free surface (as $\eta/a \rightarrow 1$). Thus, for ‘moderate’ submergence depths such as $\eta/a \approx 1.1$, three decimal places accuracy can be achieved with a value of $M = 10$, whilst for $\eta/a = 1.01$, a value of $M = 40$ was required for similar accuracy irrespective of the type of mode and in accordance with the findings of McIver and Evans [5]. In fact, the same rules regarding the choice of M were found to apply for multiple cylinders

however they are situated with respect to each other, the truncation parameter being determined in this case by the cylinder closest to the free surface. In all cases, the coefficients were scaled by $\tilde{A}_m^j = \varepsilon_m K'_m(ka_j) A_m^j$, $\tilde{B}_m^j = \varepsilon_m K'_m(ka_j) B_m^j$, giving a system whose determinant is of $O(1)$ for all M .

We expect the trapped mode frequencies for multiple cylinders to approach those for each of the individual cylinders in isolation as the cylinders are moved far enough apart. Such a situation arose in the consideration of trapped mode frequencies about multiple vertical cylinders in uniform channels by the same authors (see [7]). It is therefore necessary to establish results for trapped mode frequencies due to a single submerged horizontal cylinder. McIver and Evans [5] computed modes which were symmetric about the vertical plane containing the centre of the cylinder, using Ursell's [1] original multipole formulation. Ursell had previously *proved* that such a symmetric trapped mode exists for sufficiently small cylinders, basing his proof on the multipole formulation. McIver and Evans [5] found that as the cylinder approaches the free surface, then further modes were present. Indeed, the second mode was estimated to occur at a submergence depth to cylinder radius ratio of $\eta/a \approx 1.07$. As [1] pointed out, the proof of the existence of an antisymmetric trapped mode fails when using the multipole construction of the solution. However, we find numerically that they exist and interlace with the symmetric trapped mode results of [5] such that there is an increasing number of modes as the cylinder moves closer to the free surface. Figures 2, 3 and 4 show the dispersion relation satisfied by the trapped modes for the submergence depths of $\eta/a = 1.10$, 1.05 and 1.01, respectively. There is at least one symmetric and one antisymmetric trapped mode in all three figures. Our computations suggest that an antisymmetric mode exists provided the depth to radius ratio, $\eta/a \lesssim 1.18$. In Figure 3, where $\eta/a = 1.05$ it can be seen that a second symmetric mode has appeared and in Figure 4, where $\eta/a = 1.01$, a second antisymmetric mode is clearly present also. A third symmetric mode cuts in through $K/k = 1$ close to $ka = 5$ although hardly visible in Figure 4, and in fact for this submergence depth there are a total of four symmetric modes interlaced with three antisymmetric modes, the remainder of which all occur at higher values of ka than are shown in Figure 4). Martin [6] has also reported obtaining antisymmetric modes numerically for both circular and elliptic cylinders.

In order to illustrate the form that both modes take, we examine the free-surface elevation when $\eta/a = 1.01$ and $ka = 3$. Then from Figure 4 with these parameters, we can see there are four modes present, two symmetric and two antisymmetric. The free surface profiles associated with these four modes are illustrated in Figure 5. As was noted in [5] the mode number is characterised by the number of zero crossings or nodes. Thus the first symmetric mode has no zero crossings, the second symmetric mode one crossing and so on, whilst the same is true of antisymmetric modes once the node at $x = 0$ has been discounted. The reader is directed to [5] for a more detailed discussion of trapped modes above a single cylinder, there being no other fundamental qualitative difference between the two types of mode. The main conclusions from their work was the following. For a fixed frequency, the effect of increasing the depth of submergence was to spread out the mode shape. The mode remains fairly localised to the cylinder apart from when a mode frequency is close to the cut-off (K/k close to unity).

3.2. MULTIPLE CYLINDERS

We shall use the results for the single cylinder to draw conclusions regarding trapped modes in the presence of more than one cylinder. There are clearly a vast number of results which can be obtained in the case of multiple cylinders with the large range of parameters we have

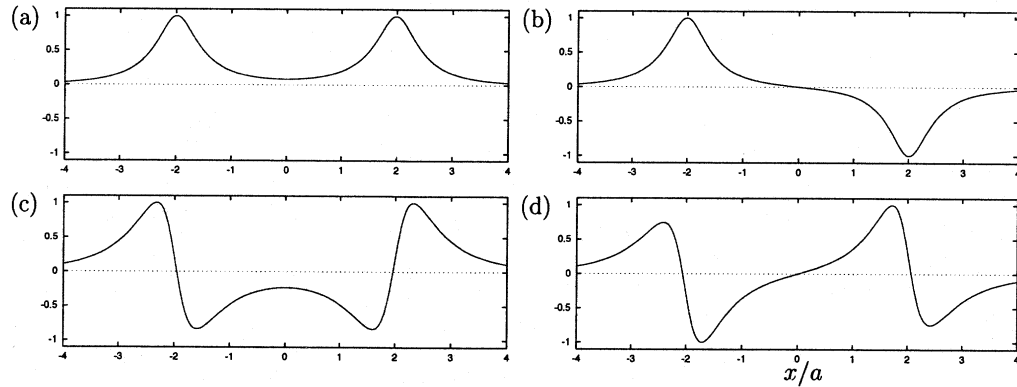


Figure 7. The free surface elevation corresponding to the four trapped modes present at $ka = 1$ and for $\eta/a = 1.05$. (a) symmetric/symmetric, (b) symmetric/antisymmetric, (c) antisymmetric/symmetric, (d) antisymmetric/antisymmetric.

at our disposal. We will concentrate primarily on the case of two cylinders and in particular, when the two cylinders are of equal size, since there are still many questions we may ask about the behaviour of the trapped modes. It is convenient to introduce a spacing parameter similar to [7] by writing the position of the two cylinder centres as $(\pm\lambda a, \eta)$. Then λ controls the separation of the cylinders with $\lambda = 1$ equivalent to the two cylinders touching. It should be noted that the numerical results for the full general system for N cylinders given by (2.23), (2.24) were cross-checked against the results for the simplified systems (2.25), (2.26) and (2.30), (2.31) when advantage was taken of various symmetries to reduce the complexity of the general system.

In Figure 6 we show the variation of K/k with ka for two equal cylinders with $\eta/a = 1.05$ and with centres a distance $4a$ apart (or $\lambda = 2$). Then we see that there are six curves in the range $0 < ka \leq 5$. Because of the geometric symmetry induced by this arrangement any trapped mode solutions must be either symmetric or antisymmetric about the plane bisecting the two cylinders ($x = 0$ in this case). In order to identify the type of motion we used the system (2.30), (2.31) in which the symmetry/antisymmetry is built into the equations. This also has the advantage of reducing the computational effort incurred when using the full system.

In Figure 6 the dotted curves represent the symmetric and antisymmetric trapped modes due to a *single* cylinder placed at $\eta/a = 1.05$ as shown in previously in Figure 3. It can be seen that with each of these is associated a ‘pair’ of curves, the lower of which is symmetric about the plane $x = 0$, whilst the upper is antisymmetric. As ka , and hence the frequency, increases these curves tend to those for the single cylinder. This can be explained by the fact that as the frequency increases the motion about each of the cylinders becomes more localised and hence the influence of one cylinder on another is reduced. As a demonstration of the form that these trapped modes take, Figure 7 shows the free surface elevation at $ka = 1$, where from Figure 6, four modes exist. The modes are ordered in increasing K/k , so that the first mode to be encountered is symmetric about $x = 0$, and almost symmetric about each individual cylinder. The second mode is antisymmetric about $x = 0$, and again almost symmetrical about each of the cylinders. The third and fourth modes are symmetric and antisymmetric respectively about $x = 0$, and are almost *antisymmetric* about each of the cylinders. These observations are summarised in the caption to Figure 7.

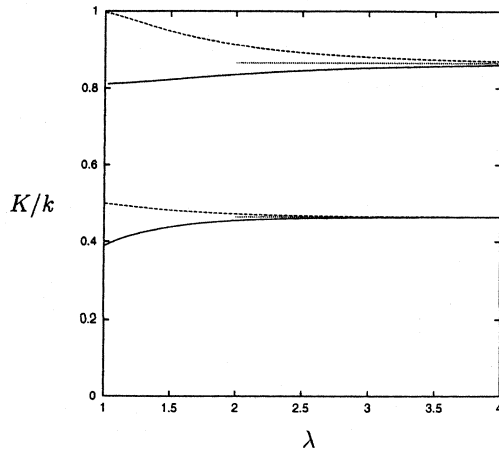


Figure 8. The variation of K/k with spacing parameter λ for two equal cylinders with $\eta/a = 1.05$, $ka = 1$: (—) symmetric and (---) antisymmetric modes, (···) single cylinder trapped modes.

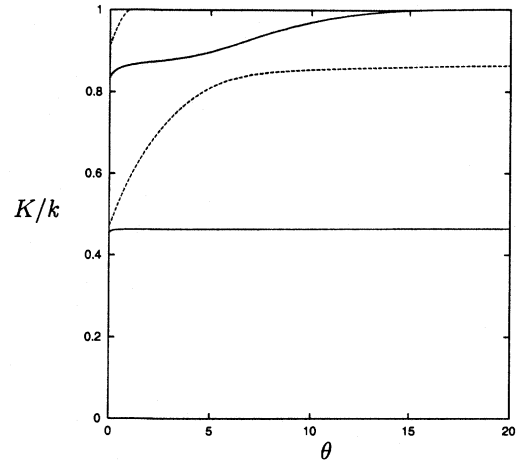


Figure 9. Curves showing the variation of K/k against θ (in degrees) for two equal cylinders as one is rotated round the other with $ka = 1$. At $\theta = 0$, $\eta_1/a = \eta_2/a = 1.05$. (—) associated with initially symmetric modes and (---) associated with initially antisymmetric modes.

In Figure 8 we show how the curves for K/k vary with λ , the spacing parameter, as two cylinders with $\eta/a = 1.05$, initially touching, are moved apart for a value of $ka = 1$. As expected, the trapped mode frequencies tend rapidly to the values for the isolated cylinders as the two cylinders are moved apart. Again, the geometric symmetry allows solutions which are symmetric and antisymmetric about the plane $x = 0$ bisecting the two cylinders. Similar curves were observed in the case of trapped modes due to multiple vertical cylinders placed on the centreplane of a uniform width channel by Evans and Porter [7].

In all cases detailed above, there has been symmetry in the geometry. It is interesting to see how the trapped modes are affected by symmetry breaking. One particularly interesting way of looking at this is as follows. Consider two equal cylinders submerged to equal depths having both symmetric and antisymmetric trapped modes. Now rotate the centre of one of the cylinders about the centre of the second cylinder, measuring its position by θ such that $\theta = 0^\circ$ is the initial symmetric set-up and $\theta = 90^\circ$ corresponds to the first cylinder being directly below the second. Here there is also symmetry. So in going from 0° to 90° we have broken symmetry, then regained it. Again we use the case of $\eta_1/a = \eta_2/a = 1.05$, a spacing parameter of $\lambda = 2$ and $ka = 1$ as the initial set-up. It can be seen from Figure 8 that there are four modes present under these parameters, alternating between symmetric and antisymmetric as K/k increases. At $\theta = 90^\circ$ computations show that there are only two modes, one symmetric and the other antisymmetric. Thus as the cylinder is rotated about its neighbour, two of the modes must vanish and this is shown clearly in Figure 9. In fact they disappear across the cut-off $K/k = 1$ for small θ and for $\theta > 20^\circ$ the two remaining modes feel very little influence from the rotated cylinder which is now deeply submerged with respect to the fixed cylinder near the free surface.

A further example of a situation where symmetry is absent is presented in Figure 10. Here the variation of K/k against the ratio a_2/a_1 of cylinder radii is plotted when one cylinder is held fixed with $\eta_1/a_1 = 1.05$ whilst the radius of a neighbouring cylinder is shrunk, about a

fixed centre with $\lambda = 1.5$, to zero with initially $\eta_2/a_2 = 1.05$. Again from Figure 8 we can see that there are four modes initially whilst Figure 3 shows that when one of the cylinders has shrunk to zero there remain only two modes (at $ka_1 = 1$). Hence we have a similar situation to before where two modes will disappear across the cut-off $K/k = 1$. This is illustrated in Figure 10 where reading across the a_2/a_1 axis from left to right corresponds to a shrinking cylinder.

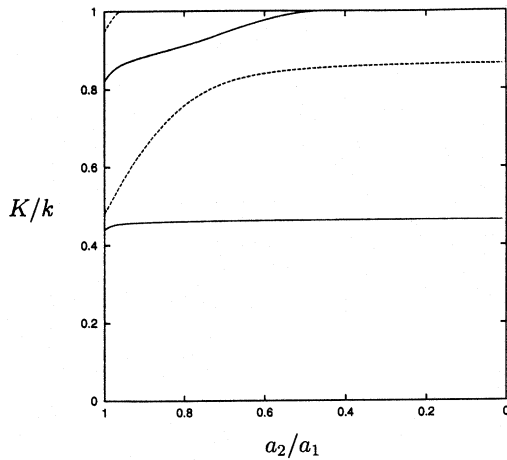


Figure 10. The variation of K/k with the ratio a_2/a_1 of cylinder radii for two cylinders, one fixed with $\eta_1/a_1 = 1.05$, and the other spaced with $\lambda = 1.5$: (—) associated with symmetric and (- - -) with antisymmetric modes.

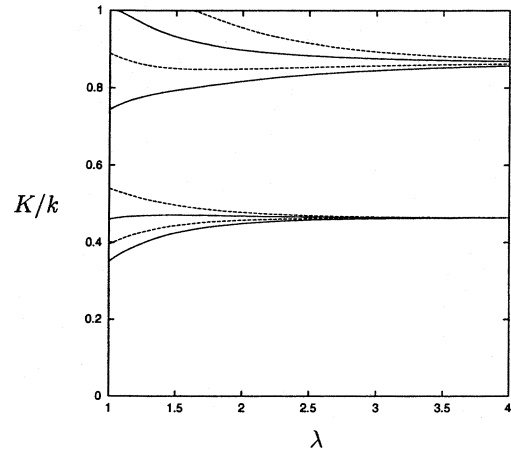


Figure 11. The variation of K/k with spacing parameter λ for four equal cylinders with $\eta/a = 1.05$, $ka = 1$: (—) symmetric and (- - -) antisymmetric modes, (\cdots) single cylinder trapped modes.

Figure 11 repeats Figure 8 but with four identical cylinders centred at $(\pm\lambda a, \eta)$, $(\pm 3\lambda a, \eta)$, and with $\eta/a = 1.05$, $ka = 1$. Initially ($\lambda = 1$) the cylinders are touching and as λ increases the cylinders are separated from their neighbours at an equal rate. Again, as they are separated the trapped mode frequencies tend to those for the cylinders in isolation. Figure 11 shows the increased number of trapped modes being squashed together with respect to K/k .

4. Conclusion

The problem of trapped surface waves above an arbitrary configuration of multiple submerged circular cylinders has been addressed. The method of solution used a combination of multipole expansion methods and addition theorems for Bessel functions to derive an infinite system of equations whose vanishing determinant as a function of various geometrical and wave parameters corresponds to a trapped mode. Results for a single cylinder have been presented, repeating those of [5] for symmetrical modes and presenting new curves of antisymmetrical modes which interlace the symmetric modes. The total number of modes depends on the ratio of cylinder size to submergence and increases as the cylinder approaches the free surface. It was found numerically that for a ratio larger than approximately 1.18 no antisymmetrical mode exists; an analytical bound on this value would appear difficult to obtain and is beyond the scope of this paper. For multiple cylinders the following conclusions can be drawn. For N ,

identical cylinders, which in isolation can support a total of Q modes, the number of modes present for large enough cylinder separations is NQ . A similar conclusion was drawn from the case of multiple cylinders in a channel considered by [7]. Furthermore, the influence of neighbouring cylinders on the trapped modes frequency of a given cylinder is small confirming the fact that trapped modes above cylinders are very local phenomena.

Appendix A. Derivation of multipoles

From Watson [9, p. 182, Equation (5)],

$$K_n(X) = \frac{1}{2} \int_{-\infty}^{\infty} e^{-X \cosh \mu - n\mu} d\mu, \quad X > 0. \quad (\text{A.1})$$

Let $X = kr'$ and make the change of variable $\mu = t + i(\pi - \theta')$. Then

$$\begin{aligned} K_n(kr') e^{-in\theta'} &= \frac{(-1)^n}{2} \int_{-\infty}^{\infty} e^{kr' \cos \theta' \cosh t} \\ &\quad \times e^{-ikr' \sin \theta' \sinh t} e^{-nt} dt, \quad \frac{1}{2}\pi < \theta' < \frac{3}{2}\pi \end{aligned} \quad (\text{A.2})$$

and we have moved the line of integration back onto the real line since $K_n(X)$, $X > 0$ is regular everywhere. We define

$$\begin{aligned} x - \xi &= r \sin \theta, & x - \xi &= r' \sin \theta', \\ y - \eta &= r \cos \theta, & y + \eta &= -r' \cos \theta', \end{aligned} \quad (\text{A.3})$$

(the subscript j is dropped throughout for ease of notation), (r, θ) being polar coordinates about (ξ, η) and (r', θ') polar coordinates, introduced for the purposes of deriving the multipoles only, about $(\xi, -\eta)$, the image of (ξ, η) in $y = 0$.

After making the substitution $n = -n$ and using the relation $K_{-n} = K_n$, we find

$$\begin{aligned} K_n(kr') e^{in\theta'} &= (-1)^n \int_0^{\infty} e^{-k(y+\eta) \cosh t} \\ &\quad \times \cosh(nt - ik(x - \xi) \sinh t) dt, \quad y > -\eta. \end{aligned} \quad (\text{A.4})$$

We write

$$w_n(r, \theta) = K_n(kr) e^{in\theta} + \int_0^{\infty} A_n(t) e^{-k(y+\eta) \cosh t} \cosh(nt - ik(x - \xi) \sinh t) dt. \quad (\text{A.5})$$

On $y = 0$,

$$\begin{aligned} \left(K + \frac{\partial}{\partial y}\right) K_n(kr) e^{in\theta} &= \left(K - \frac{\partial}{\partial y}\right) K_n(kr') e^{in\theta'} \\ &= (-1)^n \int_0^{\infty} (K + k \cosh t) e^{-k\eta \cosh t} \\ &\quad \times \cosh(nt - ik(x - \xi) \sinh t) dt, \end{aligned} \quad (\text{A.6})$$

from (A.4). So now

$$\begin{aligned} \left(K + \frac{\partial}{\partial y}\right) w_n(r, \theta)|_{y=0} &= \int_0^\infty \{(-1)^n (K + k \cosh t) + A_n(t)(K - k \cosh t)\} \\ &\quad \times e^{-k\eta \cosh t} \cosh(nt - ik(x - \eta) \sinh t) dt \\ &= 0, \end{aligned}$$

if

$$A_n(t) = (-1)^n \frac{k \cosh t + K}{k \cosh t - K}. \quad (\text{A.7})$$

So the (complex) multipoles are given by

$$\begin{aligned} w_n(r, \theta) &= K_n(kr) e^{in\theta} + (-1)^n \int_0^\infty \frac{k \cosh t + K}{k \cosh t - K} \\ &\quad \times e^{-k(y+\eta) \cosh t} \cosh(nt - ik(x - \xi) \sinh t) dt, \end{aligned} \quad (\text{A.8})$$

for $y > -\eta$. The real and imaginary parts of these form the symmetric and antisymmetric multipoles, the former of which agree with those defined in [1].

Appendix B. Shift of coordinates

In order to express $\varepsilon_n K_n(kr_j) e^{in\theta_j}$ in terms of coordinates (r_k, θ_k) , local to a cylinder k ($\neq j$), say, we use Graf's addition theorem for Bessel functions [9, p. 361, Equation (8)]. Operating with the triangle in Figure 1 having sides r_j, r_k and R_{kj} , we find that

$$K_n(kr_j) e^{in\theta_j} = \sum_{m=-\infty}^{\infty} K_{n-m}(kR_{kj}) e^{i(n-m)\alpha_{kj}} I_m(kr_k) e^{im\theta_k}. \quad (\text{B.1})$$

Taking real and imaginary parts and rearranging gives

$$\varepsilon_n K_n(kr_j) \cos n\theta_j = \sum_{m=0}^{\infty} I_m(kr_k) \{C_{mn}^{kj} \cos m\theta_k + D_{mn}^{kj} \sin m\theta_k\}, \quad (\text{B.2})$$

$$\varepsilon_n K_n(kr_j) \sin n\theta_j = \sum_{m=0}^{\infty} I_m(kr_k) \{E_{mn}^{kj} \cos m\theta_k + F_{mn}^{kj} \sin m\theta_k\}, \quad (\text{B.3})$$

where

$$C_{mn}^{kj} = \frac{1}{2} \varepsilon_n \varepsilon_m \{K_{m-n}(kR_{kj}) \cos(m-n)\alpha_{kj} + K_{m+n}(kR_{kj}) \cos(m+n)\alpha_{kj}\}, \quad (\text{B.4})$$

$$D_{mn}^{kj} = \frac{1}{2} \varepsilon_n \varepsilon_m \{K_{m-n}(kR_{kj}) \sin(m-n)\alpha_{kj} + K_{m+n}(kR_{kj}) \sin(m+n)\alpha_{kj}\}, \quad (\text{B.5})$$

$$E_{mn}^{kj} = \frac{1}{2} \varepsilon_n \varepsilon_m \{-K_{m-n}(kR_{kj}) \sin(m-n)\alpha_{kj} + K_{m+n}(kR_{kj}) \sin(m+n)\alpha_{kj}\}, \quad (\text{B.6})$$

$$F_{mn}^{kj} = \frac{1}{2} \varepsilon_n \varepsilon_m \{K_{m-n}(kR_{kj}) \cos(m-n)\alpha_{kj} - K_{m+n}(kR_{kj}) \cos(m+n)\alpha_{kj}\} \quad (\text{B.7})$$

and α_{kj} , R_{kj} are defined in (2.8), (2.9).

For the next part, we introduce the identity [10, p. 376, Equation (9.6.33)]

$$e^{(1/2)z(t+1/t)} = \sum_{m=-\infty}^{\infty} t^m I_m(z) \quad (\text{B.8})$$

and insert values of $z = -kr_k$ and $t = \exp\{u + i\theta_k\}$. Then

$$e^{-k(y-\eta_k) \cosh u} e^{-ik(x-\xi_k) \sinh u} = \sum_{m=-\infty}^{\infty} (-1)^m e^{mu} I_m(kr_k) e^{im\theta_k}, \quad (\text{B.9})$$

where (r_k, θ_k) are defined in (2.7). Also, since

$$\begin{aligned} y - \eta_j &= (\eta_k - \eta_j) + (y - \eta_k), \\ x - \xi_j &= (\eta_k - \eta_j) + (x - \xi_k), \end{aligned} \quad (\text{B.10})$$

then

$$\begin{aligned} e^{-k(y+\eta_j) \cosh u} e^{-ik(x-\xi_j) \sinh u} &= e^{-k(\eta_k+\eta_j) \cosh u} \sum_{m=-\infty}^{\infty} (-1)^m \\ &\quad \times e^{mu-ik(\xi_k-\xi_j) \sinh u} I_m(kr_k) e^{im\theta_k}. \end{aligned} \quad (\text{B.11})$$

Taking real and imaginary parts, we have

$$\begin{aligned} e^{-k(y+\eta_j) \cosh u} \cos(k(x - \xi_j) \sinh u) \\ = \sum_{m=0}^{\infty} I_m(kr_k) \{c_m^{kj}(u) \cos m\theta_k + d_m^{kj}(u) \sin m\theta_k\}, \end{aligned} \quad (\text{B.12})$$

$$\begin{aligned} e^{-k(y+\eta_j) \cosh u} \sin(k(x - \xi_j) \sinh u) \\ = \sum_{m=0}^{\infty} I_m(kr_k) \{e_m^{kj}(u) \cos m\theta_k + f_m^{kj}(u) \sin m\theta_k\}, \end{aligned} \quad (\text{B.13})$$

where

$$c_m^{kj}(u) = \varepsilon_m (-1)^m e^{-k(\eta_k+\eta_j) \cosh u} \cosh mu \cos(k(\xi_k - \xi_j) \sinh u), \quad (\text{B.14})$$

$$d_m^{kj}(u) = \varepsilon_m (-1)^m e^{-k(\eta_k+\eta_j) \cosh u} \sinh mu \sin(k(\xi_k - \xi_j) \sinh u), \quad (\text{B.15})$$

$$e_m^{kj}(u) = \varepsilon_m (-1)^m e^{-k(\eta_k+\eta_j) \cosh u} \cosh mu \sin(k(\xi_k - \xi_j) \sinh u), \quad (\text{B.16})$$

$$f_m^{kj}(u) = -\varepsilon_m (-1)^m e^{-k(\eta_k+\eta_j) \cosh u} \sinh mu \cos(k(\xi_k - \xi_j) \sinh u). \quad (\text{B.17})$$

Acknowledgements

R. P. would like to acknowledge support from EPSRC research grant no. GR/K67526.

References

1. F. Ursell, Trapping modes in the theory of surface waves. *Proc. Camb. Phil. Soc.* 47 (1951) 347–358.
2. D. S. Jones, The eigenvalues of $\nabla^2 u + \lambda u$ when the boundary conditions are given on semi-infinite domains. *Proc. Camb. Phil. Soc.* 49 (1953) 668–684.
3. F. Ursell, Mathematical aspects of trapping modes in the theory of surface waves. *J. Fluid Mech.* 183 (1987) 421–437.
4. D. V. Evans and N. G. Kuznetsov, Trapped modes. In: J. N. Hunt (ed.) *Gravity Waves in Water of Finite Depth*. Southampton: Computational Mechanics Publications (1997) pp. 127–168.
5. P. McIver and D. V. Evans, The trapping of surface waves above a submerged horizontal cylinders. *J. Fluid Mech.* 151 (1985) 243–255.
6. P. A. Martin, On the computation and excitation of trapping modes. *Proc. 4th Int. Workshop on Water Waves and Floating Bodies*, Øystose, Norway (1989) 145–147.
7. D. V. Evans and R. Porter, Trapped modes about multiple cylinders in a channel. *J. Fluid Mech.* 339 (1997) 331–356.
8. C. M. Linton and P. McIver, The scattering of water waves by an array of circular cylinders in a channel. *J. Eng. Maths.* 30 (1996) 661–682.
9. G. N. Watson, *A Treatise on the Theory of Bessel Functions*, 2nd ed. Cambridge: University Press (1966) 804 pp.
10. M. Abramowitz, and I. A. Stegun, *Handbook of Mathematical Functions*. New York: Dover (1965) 1046 pp.